J. Biomechanics Vol. 20, No. 9, pp. 851–862, 1987.
Printed in Great Britain

0021–9290/87 $3.00 + .00
Pergamon Journals Ltd.

MINIMIZATION OF THE GLIDING INDEX: CRITERION FOR THE GENERATION OF THE SURFACES OF A KNEE ENDOPROSTHESIS

J. MIZRAHI and E. BENAIM

Department of Biomedical Engineering, Technion-Israel Institute of Technology, Haifa 32000, Israel

Abstract—Previous studies on removed failed artificial knees revealed significant degradation of the articular surfaces, including pitting and shredding, as well as burnishing accompanied by score marks and scratches, the latter damage group being related to the gliding motion of the joint. In an attempt to introduce an improved version of an artificial knee joint, we have proposed a general model by which the opposing surfaces of the prosthesis components can be synthesized. The criterion applied was that of minimization of a defined gliding index. The femoral condyles in this model were expressed in terms of torus geometry, and the kinematics of motion fed into the model was that of normal motion in the sagittal plane, including angles as well as the displacement vector in the knee joint. Geometry of the tibial component was obtained from the tangents of the femoral surface, in subsequent positions of motion. The optimal surfaces were those for which the gliding index assumed a minimal value. The solutions obtained for various input motions are presented and discussed.

INTRODUCTION

The main objectives of knee joint replacement are to reduce pain and to restore normal movement capacity, without damaging other healthy functions of the body. In designing knee endoprostheses, emphasis can be put either on restoring normal kinematics of the knee (Buchanan *et al.*, 1982; Convery *et al.*, 1980; Gschwend and Loehr, 1981; Jones *et al.*, 1981; Moreland *et al.*, 1979), or on closely imitating the geometry of the natural joint (Ewald *et al.*, 1984; Finerman *et al.*, 1979; Insall *et al.*, 1979; Laskin, 1981). In the former case the resulting geometry of the prosthesis surfaces may be considerably different from that of the natural joint (Gschwend and Loehr, 1981).

In the commonly used types of artificial knee joints the contacting surfaces are to various extents non-conforming and the resulting motion is a combination of rolling and gliding (Walker *et al.*, 1981). Failure of knee joint prostheses requiring removal and subsequent revision was reported to be related primarily to loosening (e.g. Andersen, 1979; Ducheyne *et al.*, 1978; Insall, 1984; Moreland *et al.* 1979; Sledge and Walker, 1984). However, study of the removed artificial knees revealed significant degradation of the articular surfaces, greatly exceeding that observed in removed total hips in comparable time periods (Landy and Walker, 1985; Walker *et al.* 1981; Walker, 1977). Several modes of surface damage were reported, including surface wear, permanent deformation and fracture (Wright *et al.* 1985, 1982). Pitting and shredding of the surface was associated with a three-body wear mechanism as a result of ingress of cement or polyethylene particles (Bartel *et al.*, 1985; Hood *et al.*, 1983; Walker *et al.*, 1981) between the metal and the plastic components, in an environment of high contact stresses causing plastic deformation and fatigue failure of the surface (Hood *et al.*, 1981). The observed wear rate was reported to be positively correlated to the patient's body weight and time of implantation.

Another reported and significant mode of surface damage was that of abrasion and adhesion. Landy and Walker (1985) observed this type to be the most common pattern of wear (observed in 81 out of a total of 84 components examined). Burnishing and polishing in the gliding direction were noticed, accompanied by loss of material, score marks and scratches (Walker and Hsieh, 1977; Walker, 1977). Whereas the pitting and shredding modes of surface damage are strongly dominated by the contact stress magnitudes, abrasion and adhesion are clearly affected by the gliding motion as well.

In this study minimization of a defined gliding index, related to the tangential relative motion, was applied as a criterion for the generation of the opposing surfaces of a knee endoprosthesis. A general model was developed and further adapted for surfaces which are analytically expressible and was explicitly presented for the particular case where the femoral condyle surfaces were expressed in terms of torus parameters. The kinematics of motion fed into the model was that of normal motion in the sagittal plane, including the angles of the thigh and shank, as well as the displacement vector within the knee joint. An optoelectronic system was set-up in order to obtain data on various motions, not available from the literature. This paper presents the model developed, the kinematics measured and the results obtained for the geometrical parameters of the mating surfaces of the endoprosthesis.

Received 7 *March* 1986; *in revised form* 29 *September* 1986.

THE MODEL

Definition of the gliding index

Let U be a point of contact on the mating surfaces of the artificial knee ($\bar{U}$ and $\frac{\partial \bar{U}}{\partial t}$ the position and velocity vectors, respectively). For each motion k, and at a given time t a purely kinematic index element, per unit length at point U is defined as

$$G_k(t,u) = \left|\frac{\partial \bar{U}}{\partial t}\right|. \tag{1}$$

Integrating for all points of a contact curve of length $L_k(t)$, we get

$$G_k(t) = \left(\int_{L_k} G_k(t,u)\,du\right)/L_k(t). \tag{2}$$

Thus for the motion K with time T_k, the above relation is normalized

$$G_k = \left(\int_{T_k} G_k(t)\,dt\right)/T_k. \tag{3}$$

The gliding index is, therefore, obtained by the relation

$$G = \sum_k P_k G_k \tag{4}$$

where P_k denotes the occurrence of motion k in daily life activity (McLeod *et al.*, 1975).

Geometry

The surfaces of the femoral component were parameterized by means of two different tori. The simplistic torus geometry is especially convenient since it is analytically expressible by means of three parameters only. A method for the more accurate and refined representation of natural knee joint geometry was recently reported by Huiskes *et al.* (1985).

The first step for modelling the femoral condyles as tori and expressing the anatomical constraints consisted of setting the femoral and tibial reference systems, and defining the main dimension parameters of the knee (Figs 1 and 2) and their relationships to the torus parameters. This procedure is described for the tibial plateau and for the condyles of the right knee only, but can be easily extended to include the left knee as well.

Referring to Fig. 1, the femoral reference axes were defined as follows: Z_F coincides with the axis of the femoral shaft (perpendicular to the plane of the figure), X_F is parallel to the contact axis of the condyles with the tibial plateau when the femur is flexed at 90° and passing through the top point, at mid-width of the intercondylar notch, where the origin of the system is fixed. The Y_F axis is defined accordingly to form an orthogonal system. The system thus obtained is essentially similar to previously defined reference systems for the femoral condyles (e.g. Chao, 1980; Grood and Suntay, 1983), except for the following two minor differences: (a) rather than passing through the centre of the femoral head, definition of the Z_F axis in this study as parallel to the femoral shaft, allows the possibility to refer to the geometrical data supplied by Erkman and Walker (1974); (b) location of the origin in the centre of the intercondylar notch allows easier reference to the dimensions supplied by Mensch and Amstutz (1975).

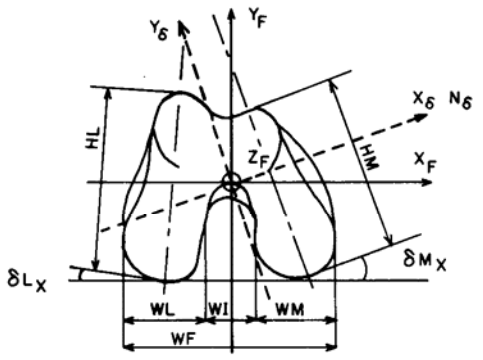

Fig. 1. Definition of the femoral reference system and dimension parameters for the femoral condyles in a 90° flexed position of the femur.

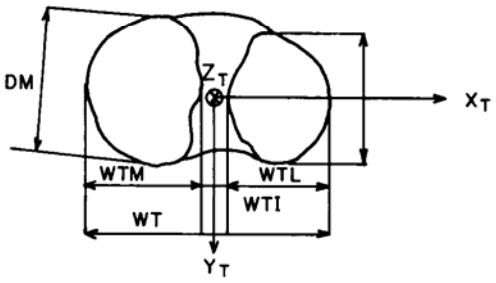

Fig. 2. Definition of the tibial reference system and dimension parameters for the tibial plateau.

A tibial reference, required to express the motion of the femur relative to the tibia was defined in a somewhat simpler way to that reported earlier by Grood and Suntay (1983): Z_T coincides with the axis of the tibia and pointing downwards, X_T sidewards and Y_T forwards (Fig. 2).

The geometrical similarity among the knees of the various individuals, as reported in the literature (Erkman and Walker, 1974; Mensch and Amstutz, 1975), has led to the suggestion that altogether four size groups of artificial knee prostheses are required to satisfy the needs of the vast majority of the population (Seedhom *et al.* 1974). Actual natural dimensions of the knee for any of these groups were thus taken from this literature.

The detailed dimensions of the femoral condyles as taken from the literature for two extreme sizes of the knee joint, the smallest and the biggest sizes, are given in Table 1. The parameters are nondimensionalized by normalization with respect to the joint's width, as suggested by Seedhom *et al.* (1972). The detailed dimensions of the tibial plateau are given in Table 2 for two extreme sizes, the smallest and the biggest.

Table 1. Detailed dimensions of femoral condyle and of torus parameters, used in the model for two extreme sizes (a = smallest, b = biggest). Values marked by an asterisk* were obtained from measurements made in this study on cadaver femora. Definition of parameters is given in Figs 1, 2 and 3.

	Ratio of anatomical and torus dimensions to width of femur (WF)				Dimensions (mm) for two extreme sizes	
	Mensch and Amstutz (1975)	Erkman and Walker (1974)	Seedhom *et al.* (1974)	Average used*	*a*	*b*
WF (Seedhom *et al.*, 1974)	1	1	1	1	71	94
WI	0.263		0.266	0.265	19	25
Medial condyle						
WM	0.354		0.369	0.36	25	34
HM	0.860		0.870	0.865	61	81
HPM		0.606		0.61	43	57
rM				0.50	35	47
DM	0.286	0.310		0.31	22	29
OMx				0.31*	22	29
OMy				−0.18*	−13	−17
OMz				−0.45*	−32	−43
RM				+0.45*	+32	+43
δMx					20°	
βM					150°	
αM					21°	
Lateral condyle						
WL	0.385		0.362	0.375	27	35
HL	0.864		0.887	0.88	62	83
HPL		0.542		0.54	38	51
rL				0.50	35	47
DL	0.296	0.312		0.33	23	31
OLx				−0.32*	−23	−30
OLy				−0.10*	− 7	− 9
OLz				−0.46*	−33	−43
RL				0.46*	33	43
δLx					5°	
βL					150°	
αL					22°	

Table 2. Detailed dimensions of tibial plateau for two extreme sizes (a = smallest, b = biggest). Definition of parameters is given in Fig. 4.

	Ratio of anatomical dimensions to width of femur (WF)				Dimensions (mm) for two extreme sizes	
	Mensch and Amstutz (1975)	Erkman and Walker (1974)	Seedhom *et al.* (1974)	Average used	*a*	*b*
WF (Seedhom *et al.*, 1974)	1	1	1	1	71	94
WT	0.992	0.991	0.984	0.990	70	93
WTM	0.404	0.395	—	0.400	28	38
WTI	0.163	0.166	—	0.165	12	16
WTL	0.426	0.438	—	0.430	31	40
DM	0.650	—	—	0.650	46	61
DL	0.608	—	—	0.608	43	57

The geometry of the torus is entirely defined by its external (R) and internal (r) radius (Fig. 3). Its position is obtained by the location of the centre of the external circle (0) and by the normal axis (X_δ) to the plane of the circle. In this notation the subscript refers to the torus system. A system of reference ($0, X_\delta, Y_\delta, Z_\delta$) is fixed onto the torus and the relation of this system to the earlier defined femoral system is shown in Fig. 4. In

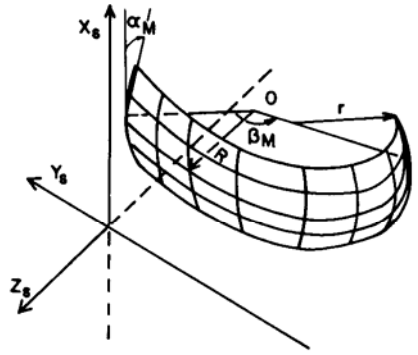

Fig. 3. Definition of parameters of the torus, used to represent the femoral surfaces.

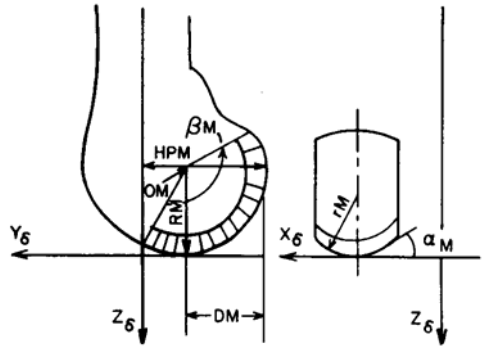

Fig. 4. Definition of the torus reference system and dimension parameters of the medial condyle.

this torus system a point U is located by its position vector $\bar{U}_\delta$ satisfying the following:

$$\begin{aligned} U_{\delta x} &= r\cos\alpha \\ U_{\delta y} &= (R-r+r\sin\alpha)\cos\beta \\ U_{\delta z} &= (R-r+r\sin\alpha)\sin\beta \end{aligned} \tag{5}$$

where α and β represent the angular positions on the internal and external circles, respectively. The parametric equations (5) of the torus are equivalent to the following implicit relation

$$F(U_\delta) = (U_{\delta x}^2 + U_{\delta y}^2 + U_{\delta z}^2 - (R-r)^2 - r^2)^2 + 4(U_{\delta x}^2 - r^2)(R-r)^2 = 0. \tag{6}$$

The position of U relative to the femoral system is obtained by the position vector $\bar{U}_f$ satisfying the relation

$$\bar{U}_f = M_\delta(\bar{O} + \bar{U}_\delta) \tag{7}$$

where M_δ is the matrix of transformation from the femoral system to the torus system. Dimensions for the torus, such as the internal radius (Fig. 4) were not available from the literature and were obtained from measurements made in this study on cadaver femora (Table 1). The centre of the internal circle was located at mid-width of the condyle. The values of α_M and β_M which define the range of the α and β parameters were determined from the relationship

$$\sin\alpha_M = \frac{WM}{Z_{rM}}. \tag{8}$$

The parameters R, r, $\bar{O}$, $\bar{X}_\delta$, were normalised to the joint's width, as suggested by Seedhom *et al.* (1972). The range of these parameters and the variables α and β were limited by the anatomical and physiological conditions, by which: (a) the dimensions of the prosthesis surfaces should be enclosed within the range of the natural knee dimensions, and (b) bone resections should be minimal. Other conditions, e.g. related to stability, laxity and stress concentration were not considered in the present study.

Formulation of the above anatomical and physiological conditions

The first of the above conditions is that the artificial surface should be restricted within the torus description of the condyles. If the index M denotes the torus parameters of the medial condyle, then by expressing the equation of the natural condyle in its implicit form (6) and describing the artifical surface through the parametric equations (5), the following inequality results

$$\begin{aligned} &\{(O_x - OM_x + r\cos\alpha)^2 \\ &\quad + (O_y - OM_y + (R-r+r\sin\alpha)\cos\beta)^2 \\ &\quad + (O_z - OM_z + [R-r+r\sin\alpha]\sin\beta)^2 - (RM \\ &\quad - rM)^2 - rM^2)^2 \\ &\quad \leqslant 4\{rM^2 - (O_x - OM_x + r\cos\alpha)^2\}\{RM - rM\}^2. \end{aligned} \tag{9}$$

The second of the above conditions may be expressed in a similar form: the artificial surface points should be outside another torus, smaller than the torus describing the natural knee. The difference between the two represents bone resection. This difference must be calculated while taking into account the thickness of the prosthesis. The signs of the inequality and of R_M are reversed in the second anatomical condition.

Finally, it should be added that the tibial surface generated should be within the dimensions given in Table 2.

Kinematics

Natural kinematics for the relative motion of the femur to the tibia for various daily motions was obtained experimentally to determine the two relations

$$\bar{U}_t = M_t\bar{U}_f + \bar{O}_t \tag{10}$$

$$d\bar{U}_t/dt = d\bar{O}_t/dt + \bar{w}\times\bar{O}_t\bar{U}_t \tag{11}$$

where U is a point fixed to the femur with the position vectors $\bar{U}_f$ in the moving femoral system, and $\bar{U}_t$, at time t, in the fixed tibial system, $\bar{w}$ is the instantaneous rotation vector, $\bar{O}_t$ is the position of the origin of the femoral system relative to the tibial system at time t, and M_t is the matrix of transformation, determined by

Euler's angles, from the tibial system to the femoral system. The Euler's angles were defined in a similar way as defined by Chao *et al.* (1983), so that ψ stands for flexion–extension, θ for abduction–adduction, and ϕ for external or internal rotation. Hence,

$$M_t = M\psi\, M\theta\, M\phi = \begin{bmatrix} \cos\phi\cos\theta & \cos\phi\sin\theta\sin\psi - \sin\phi\cos\psi & \cos\phi\sin\theta\cos\psi + \sin\phi\sin\psi \\ \sin\phi\cos\theta & \sin\phi\sin\theta\sin\psi + \cos\phi\cos\psi & \sin\phi\sin\theta\cos\psi - \cos\phi\sin\psi \\ -\sin\theta & \cos\theta\sin\psi & \cos\theta\cos\psi \end{bmatrix} \quad (12)$$

The instantaneous rotation vector $\bar{w}$, described by its components p, q and r in the tibial reference system is also related to the Euler's angles by the relations (Darboux, 1914);

$$\begin{aligned} p &= -\sin\theta\frac{d\phi}{dt} + \frac{d\psi}{dt} \\ q &= \sin\psi\cos\theta\frac{d\phi}{dt} + \cos\psi\frac{d\theta}{dt} \\ r &= \cos\psi\cos\theta\frac{d\phi}{dt} - \sin\psi\frac{d\theta}{dt}. \end{aligned} \quad (13)$$

Since U is a point on the femoral surface, with location determined by α and β, $\bar{U}_f$ must satisfy relations (7), so that at each instant t

$$\bar{U}_t = M_t M_\delta(\bar{O} + \bar{U}_\delta) + \bar{O}_t. \quad (14)$$

If U is a point of contact at instant t, its velocity should be tangent to the surfaces, so that

$$\left[\frac{\partial\bar{U}_t}{\partial\alpha} \times \frac{\partial\bar{U}_t}{\partial\beta}\right] \cdot \frac{\partial\bar{U}_t}{\partial t} = 0 \quad (15)$$

where $\partial\bar{U}_t/\partial\alpha \times \partial\bar{U}_t/\partial\beta$ is the gradient of the femoral surface at U in the tibial reference system. From equation (14) and in view of the fact that M_t, M_δ, O_t, O_δ do not depend on the variable α and β, we get that

$$\begin{aligned} \partial\bar{U}_t/\partial\alpha &= M_t M_\delta \partial\bar{U}_\delta/\partial\alpha \\ \partial U_t/\partial\beta &= M_t M_\delta \partial\bar{U}_\delta/\partial\beta. \end{aligned} \quad (16)$$

It follows that

$$\partial\bar{U}_t/\partial\alpha \times \partial\bar{U}_t/\partial\beta = M_t M_\delta(\partial\bar{U}_\delta/\partial\alpha \times \partial\bar{U}_\delta/\partial\beta). \quad (17)$$

Hence, from (11), (14) and (17), equation (15) becomes:

$$M_t M_\delta(\partial\bar{U}_\delta/\partial\alpha \times \partial\bar{U}_\delta/\partial\beta) \cdot (d\bar{O}_t/dt + \bar{w} \times M_t M_\delta (\bar{O} + \bar{U}_\delta)) = 0 \quad (18)$$

with $\bar{U}_\delta$ satisfying the relation (6). Equation (18) defines the condition for a point to be on the envelope of the femoral surface positions during motion. This envelope determines the only compatible tibial surface to this motion for the femoral surface considered. Equation (18) thus formulates the conditions for a point to be a point of contact.

Procedure for the generation of the contacting surfaces

A block diagram describing the gliding index model is given in Fig. 5. Generation of the contacting surfaces is as follows:

We denote by $\mu i(R, r, O_x, O_y, O_z, \bar{M}_\delta)$ the set of parameters which determine in the femoral system a given torus, complying with the anatomical constraints (equation 9). Different sets of torus geometries and locations are fed into the model. The natural kinematics as determined by the Euler's angles, the displacement of the origin and the instantaneous rotation vector is then applied for each set on the defined system to determine those points on the surface for which equation (18) is satisfied, i.e. the points of contact, from which the contacting tibial surfaces are actually obtained. The gliding index (equation 4) for the resulting contacting surfaces is therefore calculated for each set of parameters μ_i and the local minimum identified. The resulting optimal femoral and mating tibial surfaces are those where the minimal gliding index is obtained. In producing the tibial surface, the constraining anatomical conditions, i.e. those related to the dimensions, are enforced. The detailed procedure of calculating the contact points and subsequently the contact curves from equation (18) is shown in the flow-chart given in Fig. 6.

Consistency evaluation of the model

Reliability of the model in calculating the gliding index and in generating the points of contact was examined by introducing to it as input data parameters of the femoral torus for which the mating tibial component with zero gliding index is known. The tibial component can, on the other hand, be generated from the model and the results compared to the known surface. The motion taken as input in the model was that of pure plane rolling at constant velocity of a cylinder of radius R_o and center coordinates C_y and C_z and the plane of motion-parallel to the xy plane. Figure 7 shows the model results for these data, of the gliding index surface versus the Y and Z coordinates of the torus center. The obtained minimum of the surface plotted was indeed zero for the given specified parameters. Additionally, the opposing surface generated by the model was parallel to the xy plane (Fig. 8), and the lines of contact were evenly spaced, corresponding to the constant velocity of the given motion.

Application of the model

The above described model was applied in this study for two dimensional kinematics in the sagittal plane, for various daily activities. The more general three-dimensional kinematics (Woltring *et al.*, 1985) is more appropriate but unfortunately could not be measured in this study with sufficient accuracy. This, however, should indeed be used, once reliable and accurate data become available in the literature. The present analysis allows, however, to evaluate gliding both during the

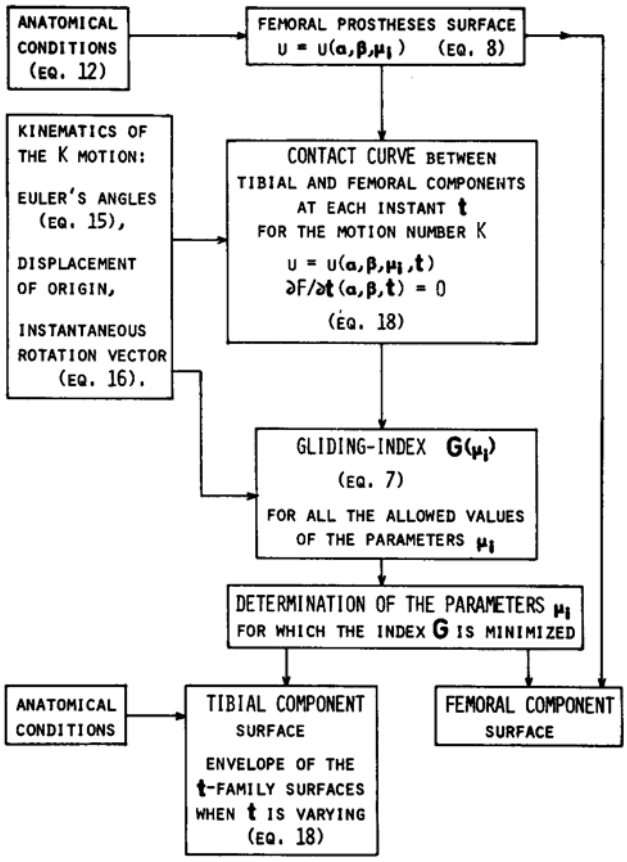

Fig. 5. Block diagram describing the gliding index model (μ_1, geometrical parameters of the femoral condyles; α, β, angle coordinates of a point on the femoral condyle surface).

design of the tibial component and also in studying the performance of existing prostheses in terms of the gliding index.

Kinematic data, which included the flexion angle, as well as the displacement vector of the knee were partly taken from the literature and partly measured in this study, as will be described in the next section. Geometrical parameters included the external radius of the torus R and the location of its centre, O_y and O_z.

EXPERIMENTAL METHOD

Sufficient data on normal gait of subjects has been reported in the literature (Chao *et al.*, 1983). In order to provide additional kinematical data for daily activities such as bending, rising, sitting and standing up, we have set up a system, initially composed of an opteoelectronic system (Selspot) and a microcomputer (Mostek Z80). A special interface including hardware and software was developed and designed for the data acquisition (Benaim, 1985). A calibration method taking account of noise, parallax error and distortion was devised by generalising already reported methods (Andriacchi *et al.*, 1979; Woltring, 1980). The much more elaborate method using a point by point calibration procedure (Mann and Antonsson, 1983), was not used in this study. Each camera–computer plane system was calibrated with reference to a calibration plane. A set of LEDs was positioned on this plane. A bipolynomial relation of variable order was assumed, the coefficients of which were obtained by minimising, for each point of interest, the difference between the real coordinate and the estimated one. Location of the camera in space, with reference to the calibration plane, was obtained as the nearest point to all lines connecting known positions of the LEDs in space and their evaluated images on the reference plane. Once the parameters of the system, namely the calibration plane coefficients and the location of the cameras, were determined, unknown objects could be located as the nearest point to the lines connecting the evaluated location of the cameras to the respective evaluated image of the object in question.

PROCEDURE

LEDs were positioned in femoral and tibial reference systems. They were attached to the leg at bony prominences, by means of elastic belts. Care was taken

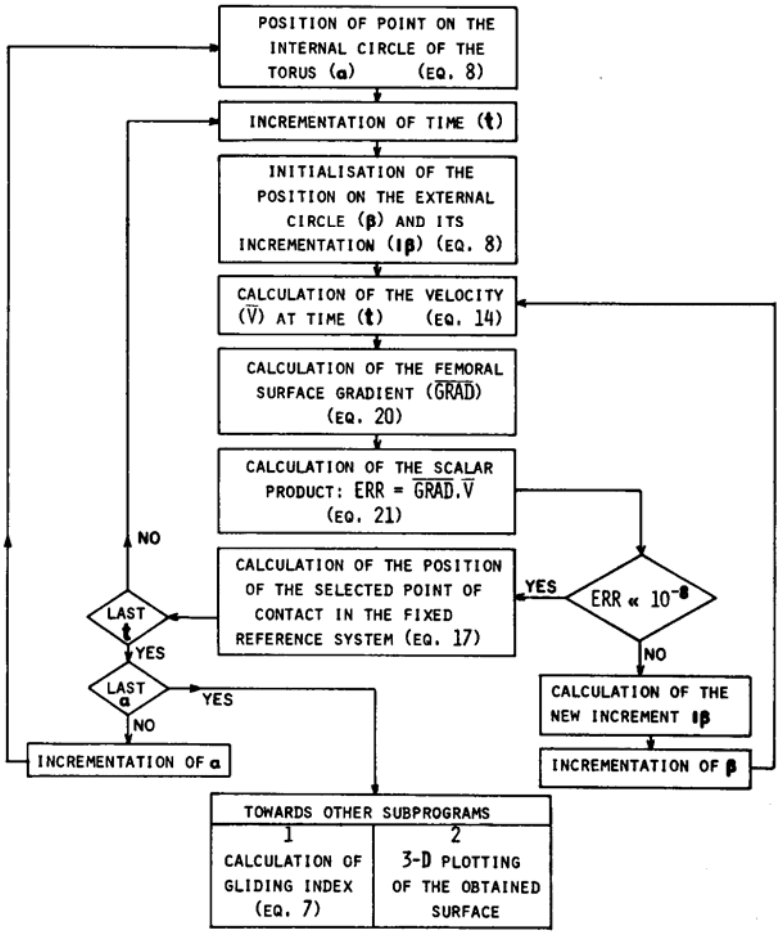

Fig. 6. Procedure of calculating contact points and contact curves from kinematics and femoral geometry.

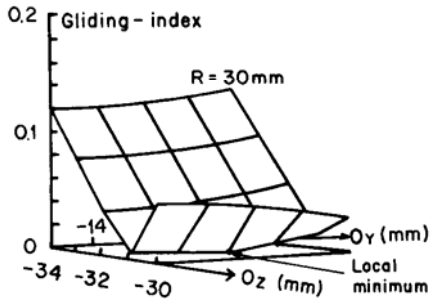

Fig. 7. Gliding-index surface obtained by introducing into the model a test motion corresponding to pure plane rolling of a cylinder at constant velocity. (R, radius of external circle; O_Y, O_Z,-coordinates of torus centre).

to properly position and attach the LEDs, with a sufficiently high preload force to reduce the soft tissue effects (Mizrahi and Susak, 1982; Streitman and Pugh, 1978; Thompson, 1973). Various daily knee motions, not previously reported in the literature, were measured for normal subjects. The motions studied are detailed in the following section. The xy coordinates were obtained for each LED as a function of time and the stick diagrams for the shank and thigh were drawn. From these diagrams the flexion angles of the knee joint were determined. The measuring accuracy of the flexion angle was 4%, believed to be within the range of individual variation of kinematics. The diplacement vector was also obtained from the stick diagrams by superimposing it on the roentgenograms of the leg of the subject.

RESULTS

Kinematics

The pattern of the different motions of the knee studied is presented in Figs 9a–f. These motions include sitting down (9a), standing up (9b), first step at gait initiation (9c), bending when using the back (9d), bending using the knees (9e) and rising from squatting position (9f). The minimal flexion angle necessary for these motions was found to be 120° (9e), which agrees with the results previously reported in the literature (Laubenthal *et al.*, 1972). These data were used as input kinematic data in the model.

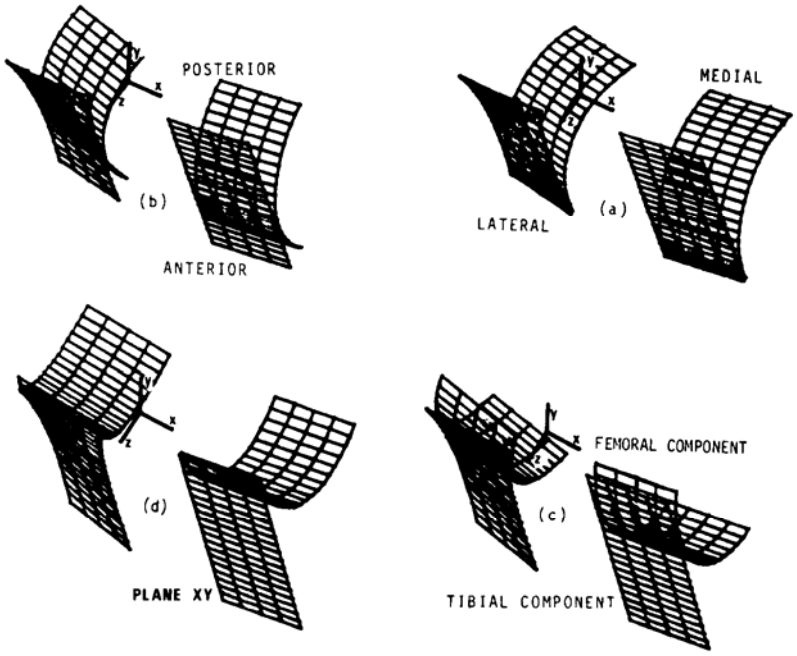

Fig. 8. Mating surfaces obtained for test motion at different positions: (a) 0°, (b) 45°, (c) 90°, (d) 120°.

Model results for daily motion

As no qualitative difference was found between the results of the medial and the lateral condyles, the results and discussions to follow will be presented for the medial condyle only.

A three-dimensional plotting of the gliding index surface as a function of the coordinates O_Y and O_Z of the centre of the torus is shown in Fig. 10 for bending motion using the knees. The gliding index surface slopes outwards, towards $+O_Z$ and in the figure two surfaces are shown, for two different values of the torus radius. It is seen from the figure that the gliding index is affected by the size of the radius of the torus and the O_Z location of its centre, and less so by its O_Y location. Thus, the gliding index is found to decrease, when increasing the radius of the torus R and at the marginal values of O_Y and O_Z (points A in Fig. 10).

When plotting the gliding index parameter for the various motion types measured earlier (Fig. 9), it was found that the general features of the plotted surfaces were the same. Although the actual gliding index values, i.e. the level of the surface above the O_Y O_Z plane, were strongly affected by the type of motion, the locations corresponding to minimum gliding index remained the same. This is demonstrated in Fig. 11, for the sitting down motions, which can be compared to the bending motion using the knees, Fig. 10.

The range of valid values of the torus parameters, i.e. those which comply with the anatomical constraints is shown in Fig. 12. Non valid values of O_Y and O_Z for given values of R were omitted from the solid surface and represented by dots. The motion for which the data in Fig. 12 are plotted corresponds to bending motion using the knees, earlier shown to have the widest knee flexion range, thus imposing more severe constraints and resulting in a narrower range of values for the torus parameters.

The optimal prosthesis surfaces for the input anatomical data are defined by means of the parameters given in Table 3. The surfaces are shown from a posterior view in different positions in Fig. 13. As seen from this figure, both tibial surfaces obtained were convex.

DISCUSSION

The model presented in this study introduces the following new concepts for the design and evaluation of knee endoprostheses: (1) Determination of design parameters for a prosthesis satisfying a given natural kinematics, by minimizing the gliding index, the latter shown to be related to adhesive and abrasive wear. (2) Generation of tibial surface from the known motion of the femoral component. (3) Evaluation of existing knee endoprostheses by means of the gliding index.

The surfaces of a 'rolling' type prosthesis were determined in this study by minimization of the gliding index. However, these could also be obtained by another method, according to which pure rolling motion is achieved by the usage of calculated incongruent surfaces (Elad *et al.*, 1981). This latter method requires the incorporation of a constraining linkage between the two surfaces of the prosthesis—hence implying sacrifice of the cruciate ligaments—to ensure that pure rolling is indeed obtained (Wongchaisuwat

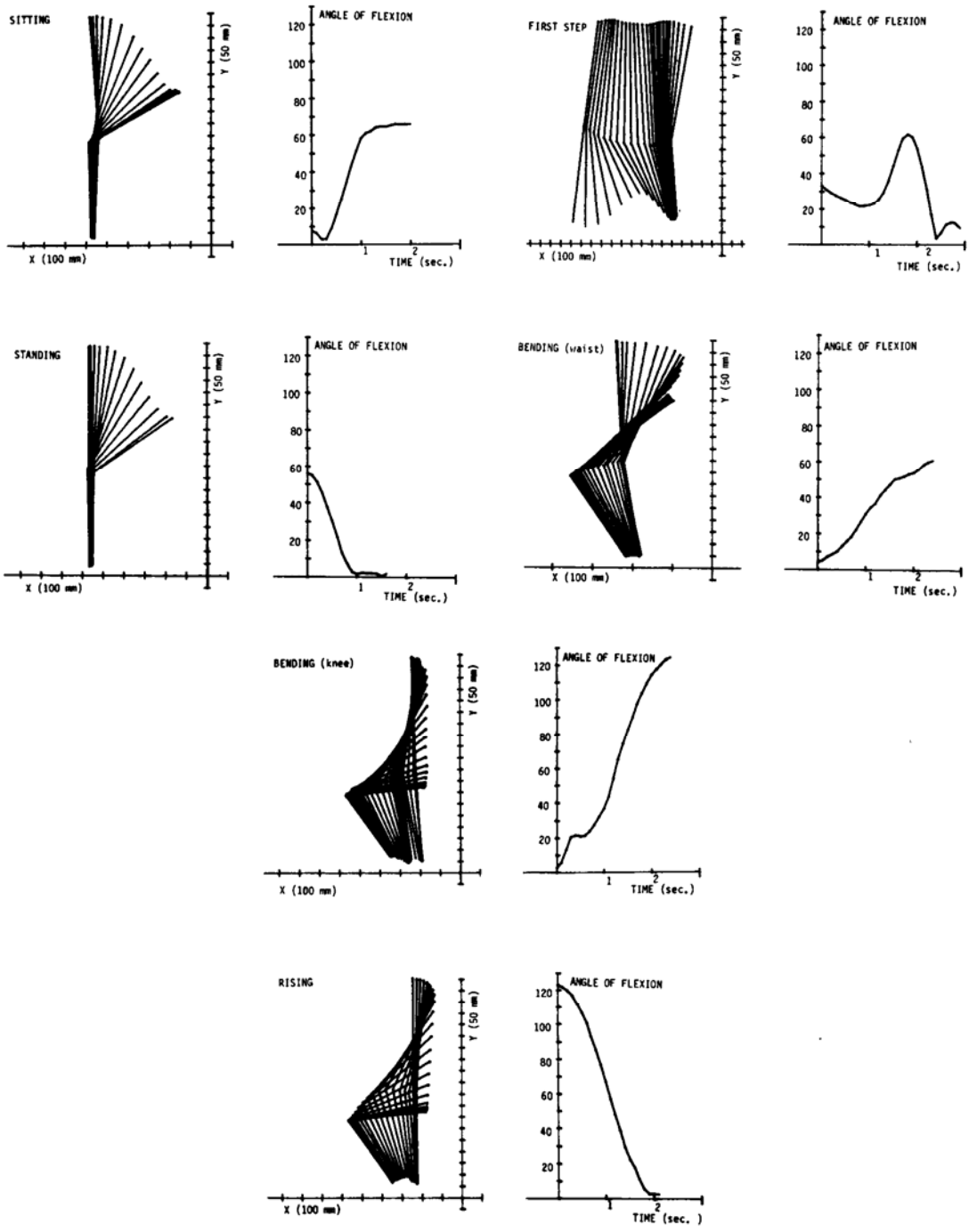

Fig. 9. Pattern of different knee motions studied: (a) sitting down, (b) standing up, (c) first step at gait inititation, (d) bending using the back, (e) bending using the knees and (f) rising from a squatting position.

et al., 1984). It should be noted, however, that with this constraining linkage, the actual prosthesis becomes exposed to higher loads and more subject to loosening.

The starting point in setting up the general model was the formulation of a gliding index (equation 1), integrated for the points on the contact curve and over the time of duration of a given motion, and weighed for the occurrence of different motions in daily life activity (equations 2–4). Geometrically the model was formulated to generate the femoral surfaces in terms of torus parameters (equations 5–7), by which the anatomical constraints were also formulated (equation 9). From the input kinematics the tibial mating surface is obtained as the envelope of the femoral surface

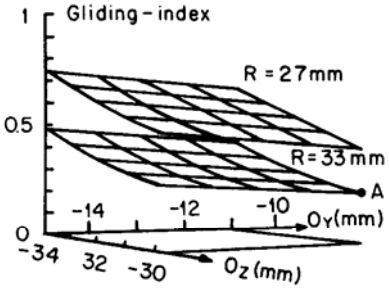

Fig. 10. Three-dimensional plotting of the gliding index surface for bending motion using the knee as a function of the coordinates O_Y and O_Z of the centre of the torus. Note that minimum value is obtained at point A, for which the gliding index is 0.2 approximately, and corresponding to $R = 33$ mm, $O_Z = -30$ mm and $O_Y = -11$ mm.

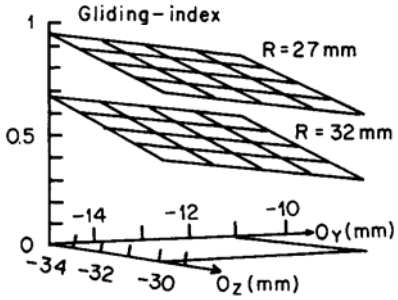

Fig. 11. Three dimensional plotting of the gliding index surface for sitting-down motions.

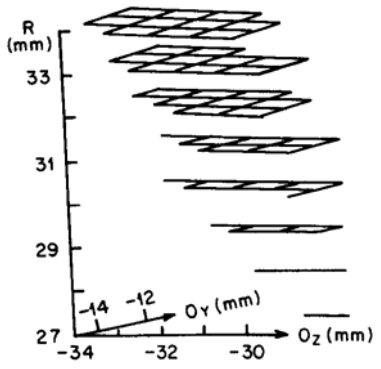

Fig. 12. Range of valid values of the torus parameters, i.e. those which comply with the anatomical constraints. Motion to which these data are given is bending using the knee.

positions during the motion. The procedure for generation of the contacting surface from the model (Figs 5, 6) was aimed at determining the surfaces for which the gliding index obtained a minimal value.

As stated earlier, application of the model was done in accordance with the data already available from the literature and the supplementary data obtained in this study. These consisted of two-dimensional kinematics in the sagittal plane for various daily activities and

Table 3. Orientation and coefficients of the optimal prostheses. The parameters are obtained by multiplying the given coefficients by the total width of the femur, taken from one of the following four groups: (1) 71 mm, (2) 78 mm, (3) 86 mm, (4) 94 mm

		Medial condyle	Lateral condyle
Orientation	δx	20°	−5°
	δy	0°	0°
	δz	0°	0°
Center	Ox	0.31	−0.32
	Oy	−0.18	−0.06
	Oz	−0.42	−0.42
Radius			
Internal	RS	0.5	0.5
External	RB	0.45	0.44

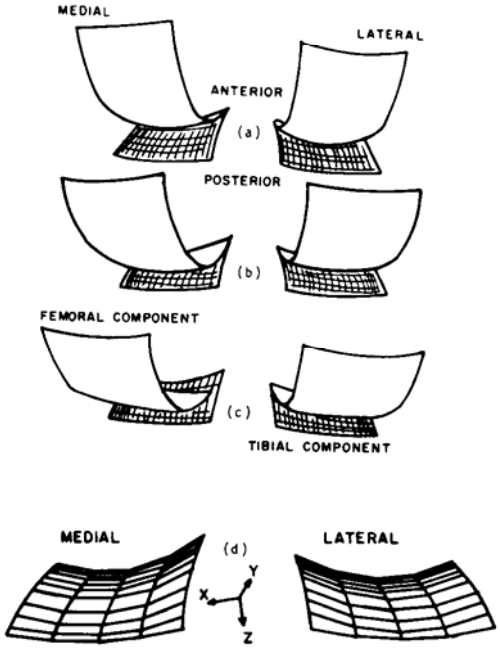

Fig. 13. Knee prosthesis surfaces shown from a posterior view in different positions: (a) 0°, (b) 30°, (c) 60°, (d) view of tibial prosthesis surfaces.

included two parameters: the flexion angle and the displacement vector of the knee. Internal/external rotation and abduction/adduction motions were not included. The results thus obtained reflect minimization of the gliding index, as far as the kinematics in the principal plane of motion is concerned. The described model presents an approach by which: (a) the tibial component surface can be generated from any given femoral surface to achieve kinematic compatibility, and (b) the mating surfaces can be selected by minimizing gliding motion.

In our model, we proposed to calculate the envelope of the femoral component in successive positions. This envelope may be used as a basis for the design of the final tibial component independently of the type of

prostheses to be used. An exception though is the linked-joint endoprostheses for which the kinematics is already provided by the prosthesis itself.

The gliding index is an objective tool which may be used in the evaluation of prostheses both at the design stage and after implantation. This requires statistical knowledge of kinematics, as well as dynamics of the knee joint, both to be determined in studies including the participation of patients. These studies should evaluate the variation of the gliding index with time, after years of implantation, while comparing different types of prostheses implanted.

The behaviour of the gliding index was similar for all input motions used, reducing the significance of the parameter of frequency of occurrence of motions in equation (4). It should, however, be remembered that the motion used was two-dimensional and that in three-dimensional motion this parameter might assume a more significant role.

The surfaces of the tibial plateau obtained in this study were both convex. In the natural joint only one surface of the tibial plateau, the lateral, is convex resulting indeed in a reduced gliding motion there. To evaluate the prosthesis obtained by minimization of the gliding index it is also necessary to compare it to existing prostheses. Reported experiments introducing different geometries for the tibial component and measuring the resulting rolling motion (Sledge and Walker, 1984) support the results found in this study.

The convexity obtained raises however the question of stability of the joint, as indeed stability should be expected in the antero-posterior direction, which is the direction of convexity. It should be remembered, however, that the results obtained correspond to the assumed constraints and optimization criteria used in this study. Other constraints, such as those related to stability, presence and laxity of the ligaments and stress concentration should be taken into consideration as additional design factors of an artificial knee joint.

The model treated is not limited to the torus type geometry and other geometries, such as ellipsoidal or analytically expressed geometry of the natural knee, may be tested as well (Huiskes *et al.*, 1985). However, torus type geometry is easily manufacturable and may already be included into a comprehensive design of the prosthesis including additional aspects such as overall geometry, implantation procedure and materials.

Acknowledgement—This study was supported by the Technion VPR Fund—W. Levenson Fund for Biomedical Engineering Research.

REFERENCES

Andersen, J. L. (1979) Knee arthroplasty in rheumatoid arthritis. An analysis of 240 case of hemi-hinge and resurfacing arthroplasties. *Acta orthop. scand.*, Suppl., **180.**

Andriacchi, T. P., Hampton, S. J., Schultz, A. B. and Galante, J. O. (1979) Three-dimensional coordinate data processing in human motion analysis. *J. biomech. Engng.* **101,** 279–283.

Bartel, D. L., Burstein, A. H., Toda, M. D. and Edwards, D. L. (1985) The effects of conformity and plastic thickness on contact stresses in metal-backed plastic implants. *J. biomech. Engng.* **107,** 193–199.

Benaim, H. E. (1985) A three-dimensional version of a rolling type knee endoprosthesis. M.Sc. Thesis, Technion-Israel Institute of Technology, Haifa, January 1985.

Buchanan, J. R., Greer, R., Bowman, L., Shearer, A. and Gallaher, K. (1982) Clinical experience with the variable axis total knee prosthesis. *J. Bone Jt Surg.* **61A,** 337–346.

Chao, E. Y. S. (1980) Justification of triaxial goniometer for the measurement of joint rotation. *J. Biomechanics* **13,** 989–1106.

Chao, E. Y. S., Laughman, R. K., Schneider, E. and Stauffer, R. N. (1983) Normative data of knee joint motion and ground reaction forces in adult level walking. *J. Biomechanics* **16,** 219–233.

Convery, F. R., Convery, M. M. and Malcom, L. L. (1980) The spherocentric knee: a re-evaluation and modification. *J. Bone Jt Surg.* **62A,** 320–327.

Darboux, G. (1914) *Theorie Generale des Surfaces* (1st part). Gauthiers–Villars, Paris.

Ducheyne, P., Kagan, A., II and Lacey, J. A. (1978) Failure of total knee arthroplasty due to loosening and deformation of the tibial component. *J. Bone Jt Surg.*, **60A,** 384–391.

Elad, D., Seliktar, R. and Mendes, D. (1981) Synthesis of a knee joint based on pure rolling. *Engng Med.* **10,** 97–105.

Erkman, M. J. and Walker, P. S. (1974) A study of knee geometry applied to the design of condylar prostheses. *Biomed. Engng* **9,** 14–17.

Ewald, F. C., Jacobs, M. A., Miegel, R. E., Walker, P. S., Poss, R. and Sledge, C. B. (1984) Kinematic total knee replacement. *J. Bone Jt Surg.* **66A,** 1032–1040.

Finerman, G. A. M., Coventry, M. B., Riley, L. H., Turner, R. H. and Upshaw, J. (1979) Anametric total knee arthroplasty. *Clin. Orthop. Rel. Res.* **145,** 85–90.

Grood, E. S. and Suntay, W. J. (1983) A joint coordinate system for the clinical description of three-dimensional motions: application to the knee. *J. biomech. Engng* **105,** 136–144.

Gschwend, N. and Loehr, J. (1981) The GSB replacement of the rheumatoid knee joint. *Reconst. Surg. Traum.* **18,** 174–194.

Hood, R. W., Wright, T. M. and Burstein, A. H. (1983) Retrieval analysis of total knee prostheses: a method and its application to 48 total condylar prostheses. *J. biomed. Mat. Res.* **17,** 829–842.

Hood, R. W., Wright, T. M., Fukubayashi, T. and Burstein, A. H. (1981) Contact area and pressure distribution in contemporary total knee designs. *Joint ASME/ASCE Mechanics Conference*, June 1981, Boulder, Colorado (Edited by Van Buskirk, W. C. and Woo, S. L.-Y.) pp. 233–234. AMD 43.

Huiskes, R., Kremers, J., DeLange, A., Woltring, H. J., Selvik, G. and van Rens, Th. J. G. (1985) Analytical stereophotogrammetric determination of three-dimensional knee-joint geometry. *J. Biomechanics* **18,** 559–570.

Insall, J. N. (1984) Total knee replacement. *Surgery of the Knee* (Edited by Insall, J. N.) pp. 587–695. Churchill Livingstone, New York.

Insall, J., Scott, W. N. and Ranawat, C. S. (1979) The total condylar knee prosthesis. A report of 220 cases. *J. Bone Jt Surg.* **61A,** 173–180.

Jones, W. T., Bryan, R. S., Peterson, L. F. A. and Ilstrup, D. M. (1981) Unicompartmental knee arthroplasty using polycentric and geometric hemicomponents. *J. Bone Jt Surg.* **63A,** 946–953.

Landy, M. and Walker, P. S. (1985) Wear in condylar replacement knees. A 10-year followup. *31st Annual Orthopaedic Research Society*, Las Vegas, Nevada, p. 96.

Laskin, R. S. (1981) Total condylar knee replacement in

rheumatoid arthritis. A review of 117 knees. *J. Bone Jt Surg.* **63A,** 29–35.

Laubenthal, K. N., Smidt, G. L. and Kettelkamp, D. B. (1972) A quantitative analysis of knee motion during activities of daily living. *Phys. Therap.* **52,** 34–41.

McLeod, P. C., Kellelkamp, D. B., Srinivasan, V. and Henderson, O. L. (1975) Measurements of the repetitive activities of the knee. *J. Biomechanics* **8,** 369–373.

Mann, R. W. and Antonsson, E. K. (1983) Gait analysis. Precise, rapid, automatic, 3-D position and orientation kinematics and dynamics. *Bull. Hosp. Joint Dis.*, **XLIII,** 137–146.

Mensch, J. S. and Amstutz, H. C. (1975) Knee morphology as a guide to knee replacement. *Clin. Orthop. Rel. Res.*, **112,** 231–241.

Mizrahi, J. and Susak, Z. (1982) *In vivo* elastic and damping response of the human leg to impact forces. *J. biomech. Engng* **104,** 63–66.

Moreland, J. R., Thomas, R. J. and Freeman, M. A. R. (1979) ICLH replacement of the knee. *Clin. Orthop. Rel. Res.* **145,** 47–59.

Seedhom, B. B., Longton, E. B., Dowson, D. and Wright, V. (1972) Dimensions of the knee. *Ann. rheum. Dis.*, **31,** 54–58.

Seedhom, B. B., Longton, E. B., Dowson, D. and Wright, V. (1974) Engineering and physiological consideration in the design of a total knee prosthesis. *Human Locomotor Engineering*, pp. 60–68. The Institution of Mechanical Engineers, London.

Sledge, C. B. and Walker, P. S. (1984) Total knee replacement in rheumatoid arthritis. *Surgery of the Knee* (Edited by Insall, J. N.) pp. 697–715. Churchill Livingstone, New York.

Streitman, A. and Pugh, J. (1978) The response of the lower extremity to impact forces. I. Design of an economical low frequency recording system for physiological waveforms. *Bull. Hosp. Joint Dis.* **XXXIX,** 63–73.

Thompson, G. A. (1973) *In vivo* determination of bone properties from mechanical impedance measurements. Aerospace Medical Association Annual Scientific Meeting, Las Vegas 7–10 May.

Walker, P. S., Ben-Dov, M., Askew, M. J. and Pugh, J. (1981) The deformation and wear of plastic components in artificial knee joints—an experimental study. *Engng Med.* **10,** 33–38.

Walker, P. S. (1977) *Human Joints and their Artificial Replacements* p. 206. Charles C. Thomas, Springfield, IL.

Walker, P. S. and Hsieh, H.-H. (1977) Conformity in condylar replacement knee prostheses. *J. Bone Jt Surg.* **59B,** 222–228.

Wright, T. M., Burstein, A. H. and Bartel, D. L. (1985) Retrieval analysis of total joint replacement components: a six-year experience. *Corrosion and Degradation of Implant Materials: Second Symposium* (Edited by Fraker, A. C. and Griffin, C. D.) pp. 415–428. American Society for Testing and Materials, Philadelphia, PA.

Wright, T. M., Hood, R. W. and Burstein, A. H. (1982) Analysis of material failures. *Orthop. Clin. N. Am.* **13,** 33–43.

Woltring, H. J. (1980) Optoelectronic (SELSPOT) gait measurement in 2 and 3-dimensional space. A Preliminary report. *Bull. prosth. Res.* **10,** 46–52.

Woltring, H. J., Huiskes, R., De Lange, A. and Veldpaus, F. E. (1985) Finite centroid and helical axis estimation from noisy landmark measurements in the study of human joint kinematics. *J. Biomechanics* **18,** 379–389.

Wongchaisuwat, C., Hemami, H. and Buchner, H. J. (1984) Control of sliding and rolling at natural joints. *J. biomech. Engng* **106,** 368–375.